

## Effects of Forming Pores on Mechanical Property of $Zr_{70}Cu_{30}$ Metallic Glass

Shidong Feng<sup>a</sup>, Pengfei Yu<sup>a</sup>, Fengli Zhao<sup>a</sup>, Likun Gao<sup>a</sup>, Na Xu<sup>a</sup>, Gong Li<sup>a,b</sup>,

Mingzhen Ma<sup>a</sup>, Li Qi<sup>a\*</sup>, Riping Liu<sup>a</sup>

<sup>a</sup>State Key Laboratory of Metastable Materials Science and Technology, Yanshan University, Qinhuangdao, 066004, P. R. China

<sup>b</sup>Department of Materials Science and Engineering, The University of Tennessee, Knoxville, Tennessee, 37996, USA

Received: September 9, 2014; Revised: September 30, 2015

Effects of forming pores in  $Zr_{70}Cu_{30}$  metallic glass on the deformation behaviour is investigated through molecular dynamics simulations. The formation of pores leads to only a small reduction in strength, but dramatically enhanced plasticity in compression. The large plasticity of glass is attributed to the large effective free space induced by forming pores. It can also promote formation of crystalline phases in the amorphous matrix during deformation. Simulation reproduces the images of the evolution of pores in the metallic glass. The simulation results are in good agreement with experimental results.

**Keywords:** pores, metallic glass, mechanical property, molecular dynamic simulation

### 1. Introduction

Bulk metallic glasses (BMGs) have several superior mechanical properties, including large elastic limits, high strengths, high hardness, and high corrosion resistance<sup>1</sup>. However, their applications are limited by falling catastrophically on one dominant shear upon uniaxial load at room temperature<sup>2,3</sup>. To alleviate this problem, many studies have been done recently to enhance their plasticity<sup>4-10</sup> by various methods such as introduction of a second phase, introduction of shear bands, and control of free volume.

With low density and special structures imparting high plasticity, foams based on BMGs have attracted much attention<sup>11,12</sup>. The foams can be fabricated by using different methods such as mixing the melt with hydrated  $B_2O_3$  in BMGs<sup>13</sup>, or holding it under pressurized hydrogen<sup>14</sup>; or by infiltration of the melt between packed crystals of NaCl salts which can then be leached out in water or acid solution<sup>15</sup>. It has been shown that dispersing pores in metallic glasses can greatly improve their plasticity. However, the reason why the pores can improve plasticity is not clear on the atomic scale.

In this study, we remove Cu atoms from  $Zr_{70}Cu_{30}$  MG via molecular dynamics simulations in order to form pores. Molecular dynamics simulations can efficiently achieve the process on the atomic scale. It was found that the forming pores can improve the glass plasticity significantly during uniaxial compression test.

### 2. Theoretical Model and Calculation Details

We introduce pores in  $Zr_{70}Cu_{30}$  MG by removing Cu atoms. ZrCu was discovered to be a binary bulk MG<sup>16</sup>. Since binary alloys are easier to model than alloys which with more elements, it makes ZrCu an attractive MG to study theoretically. The simulations are carried out using

the embedded atom method (EAM) potential<sup>17</sup> supplied in LAMMPS. The dimension of the model structures used in the calculations are  $27.5 \text{ nm} \times 5.5 \text{ nm} \times 55 \text{ nm}$ , respectively in x, y and z direction, the structures contain approximately 500 000 atoms. We first equilibrated these models with 3D periodic boundary conditions (PBCs) at 2000K, which is above the melting point of these amorphous alloys, for 1 ns. The models were then cooled at an MD cooling rate of 1 K/ps to 50 K at zero external pressure (NPT ensemble, i.e., constant number, constant pressure, and constant temperature).

In order to distinguish the original  $Zr_{70}Cu_{30}$ , we adopt  $Zr_{70}$  to stand for processed sample. Afterward, a constant and uniaxial strain rate of  $1 \times 10^{-7} \text{ fs}^{-1}$  is used at the temperature of 50 K by moving the rigid atoms at one end along the z axis, while keeping the rigid atoms at the other end unchanged. It is worth mentioning that we take the low temperature (50 K) as simulation temperature to highlight the material responses upon mechanical activation and prevent the annihilation of free volume by thermal activations<sup>18</sup>.

### 3. Result and Discussion

#### 3.1. Pair distribution function

To confirm the glassy nature, we adopt pair distribution function (PDF) to describe the structure. Figure 1a shows the PDF of  $Zr_{70}$  and  $Zr_{70}Cu_{30}$  specimen. It is obviously observed that the structure of the specimen is unaffected by the removing Cu atoms, keeping the amorphous structure suggested by splitting in the second peak of the PDF. Figure 1b shows various proportions of voronoi polyhedron (VP) coordination number, which are around Zr. It can be seen that they satisfy the Gaussian distribution, and the main VP coordination number of  $Zr_{70}$  is 11, while that of  $Zr_{70}Cu_{30}$  is 14, indicating the bigger free space in  $Zr_{70}$  specimen.

\*email: [qili@ysu.edu.cn](mailto:qili@ysu.edu.cn), [ripping@ysu.edu.cn](mailto:ripping@ysu.edu.cn)

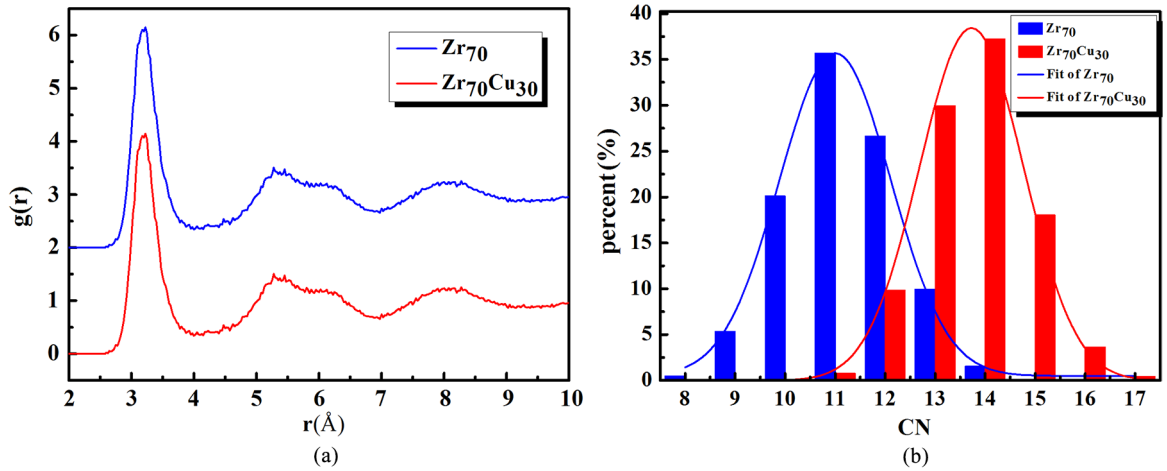


**Figure 1.** (a) The PDF of  $Zr_{70}$  MG. (b) Various proportions of voronoi polyhedron (VP) coordination number, which are around Zr.

**Table 1.** The content of each voronoi polyhedron (VP), and the corresponding volume of VP.

VP index of $Zr_{70}$	Percent %	Volume ( $\text{\AA}^3$ )	VP index of $Zr_{70}Cu_{30}$	Percent %	Volume ( $\text{\AA}^3$ )
(0,2,8,1)	8.87	29.38	(0,1,10,2)	7.69	21.73
(0,3,6,2)	6.20	29.76	(0,1,10,3)	5.53	21.91
(0,3,6,3)	6.67	29.91	(0,2,8,4)	9.77	22.17
(0,4,4,2)	6.17	31.02	(0,3,6,4)	9.54	22.06
(0,4,4,3)	8.07	30.32	(0,3,6,5)	6.21	22.41

### 3.2. Effective free space

In order to further characterizing the increased free space, we calculated the content of each VP, whose content is more than 5%, and the corresponding volume of VP, as shown in Table 1. In order to be more comparable, we propose a parameter:

$$V_e = \frac{1}{N} \sum_{i=1}^N V_i \times P_i \quad (1)$$

where  $V_e$  stands for the effective free space,  $N$  stands for the total types of VP,  $V_i$  is the volume of polyhedra type  $i$ ,  $P_i$  is the content of polyhedra type  $i$ . The  $V_e$  of  $Zr_{70}$  is 2.16, while that of  $Zr_{70}Cu_{30}$  is 1.71. We can see that after forming pores, the effective free space gets larger, and atoms have more free volume. Compared with that of the original  $Zr_{70}Cu_{30}$  MG, about 26.3% extra free space is introduced by forming pores.

### 3.3. Stress-strain curves

Figure 2 presents the compressive stress-strain curves for  $Zr_{70}$  and  $Zr_{70}Cu_{30}$  MGs. Compressive stress-strain curves are strongly affected by forming pores. For  $Zr_{70}Cu_{30}$  MG, the stress reaches 1.5 GPa and then suddenly drops. The sudden drops are caused by the formation of shear bands (SBs). However, for  $Zr_{70}$  MG, the curve does not appear sudden drop. The results demonstrate that the deformability and stability of samples produced with forming pores is significantly enhanced as compared to original samples, and it has been achieved without much degradation of strength.

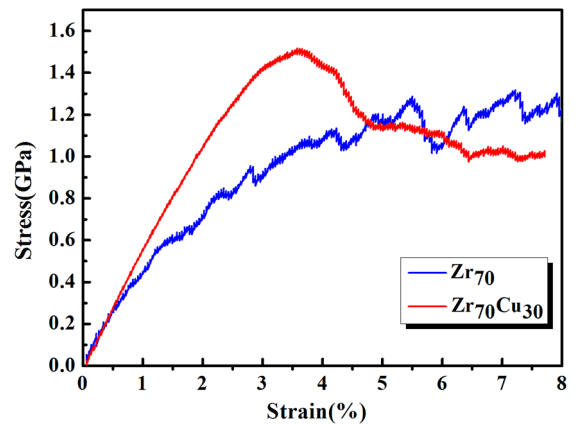


**Figure 2.** The compressive stress-strain curves for  $Zr_{70}$  and  $Zr_{70}Cu_{30}$  MGs.

### 3.4. Atomic shear strain

To better understand the mechanism of improved plasticity, systems compressed by 7% strain with atoms colored by the local value of the deviatoric shear strain  $\eta_i^{MISES}$ , corresponding to  $Zr_{70}$  and  $Zr_{70}Cu_{30}$  MGs were observed in Figure 3<sup>19</sup>. The forming porosity force the proliferation of shear bands (SBs) below the overall failure stress. Not only the quantity of SBs in (b) is more than that in (a) but also the distribution of SBs in (b) is more scattered than that in (a). Figure 3a shows the directions of

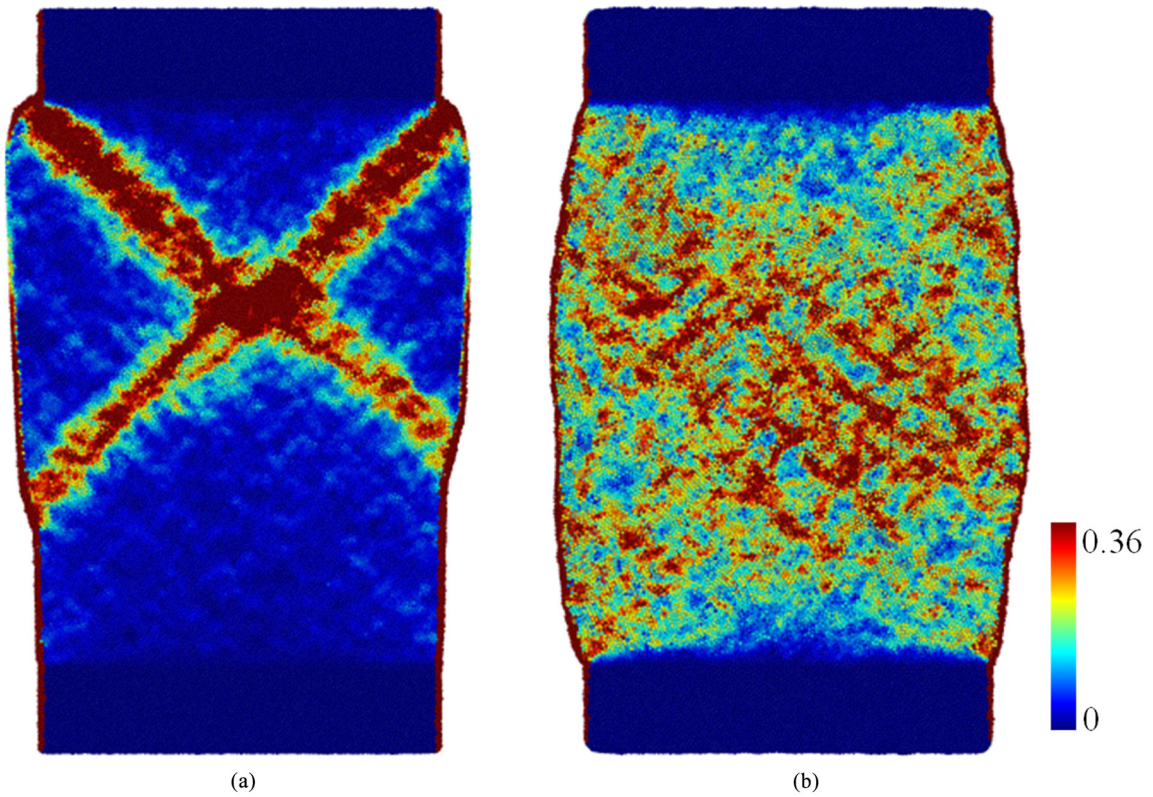


**Figure 3.** Systems compressed by 7% strain with atoms colored by the local value of the deviatoric shear strain  $\eta_v^{MISES}$ , corresponding to (a)  $Zr_{70}Cu_{30}$  and (b)  $Zr_{70}$  MGs .

the SBs are mainly  $45^\circ$  and  $135^\circ$ , while the directions of SBs in (b) are not very clear. The multishear-band pattern is usually observed in the multiaxial stress state such as that in the indentation or notched samples<sup>20</sup>. In the present study, it is realized that the deformation proceeds under the uniaxial stress mode. These differences suggest that after forming porosity, amount of SBs generate at these locations in the following uniaxial compression deformation process. The shear-band pattern is affected by the pores acting as stress concentrators. It was found that the shear bands branch and highly intersect with each other in the sample prepared by forming porosity. The high density of shear bands with the extensive interaction and branch of shear bands is closed related with plasticity enhancement, reflecting the good deforming ability of  $Zr_{70}$  MG. In contrast, the  $Zr_{70}Cu_{30}$  MG is easy to form strain location in the compressive deformation process. With increasing strain, two major SBs penetrates the system, as shown in (a). Importantly, the simulation result is in very good agreement with the experimental results<sup>21,22</sup>. Wang et al.<sup>21</sup> explained multiplication shear band formation resulting from forming porosity contributes to the improved plasticity. The difference is obviously at the composition, deformation temperature and straining conditions. However, the fact that forming porosity which prevents stress localization is well agreed between the experiment and simulation. As a

result, the initiation and propagation of a major SB that cause catastrophic shear fracture will be avoided.

In all, the large effective free space could be induced by forming pores. The nucleation of multiple shear bands owes to the large amount of randomly distributed free space, together with the branch and interaction of the shear bands, directly results in the enhancement of plastic deformation. The large amount of free space also leads to the increase of the mobility of atoms. The high mobility of atoms due to the large amount of free space remits the shear local deformation.

### 3.5. Common neighbor analysis

Figure 4 shows the common neighbor analysis (CNA) for  $Zr_{70}$  and  $Zr_{70}Cu_{30}$  MGs when strain is 7%. We can easily see that there formed the FCC and HCP crystals in  $Zr_{70}$  MG. One of the effective approaches for enhancing plasticity is the fabrication of materials consisting of an amorphous matrix with one or more crystalline phases<sup>23-25</sup>. In the process of deformation, grain nucleates and mergers induced by stress. It is analogical to crystallization by annealing. The main difference is the external cause, meaning the stress and temperature. Pores formed by removing Cu atoms are stress concentrators, and this forces atoms around pores generating crystallization. The second phase induced by porosity can effectively stabilize against the shear localization and propagation of critical shear bands upon loading.

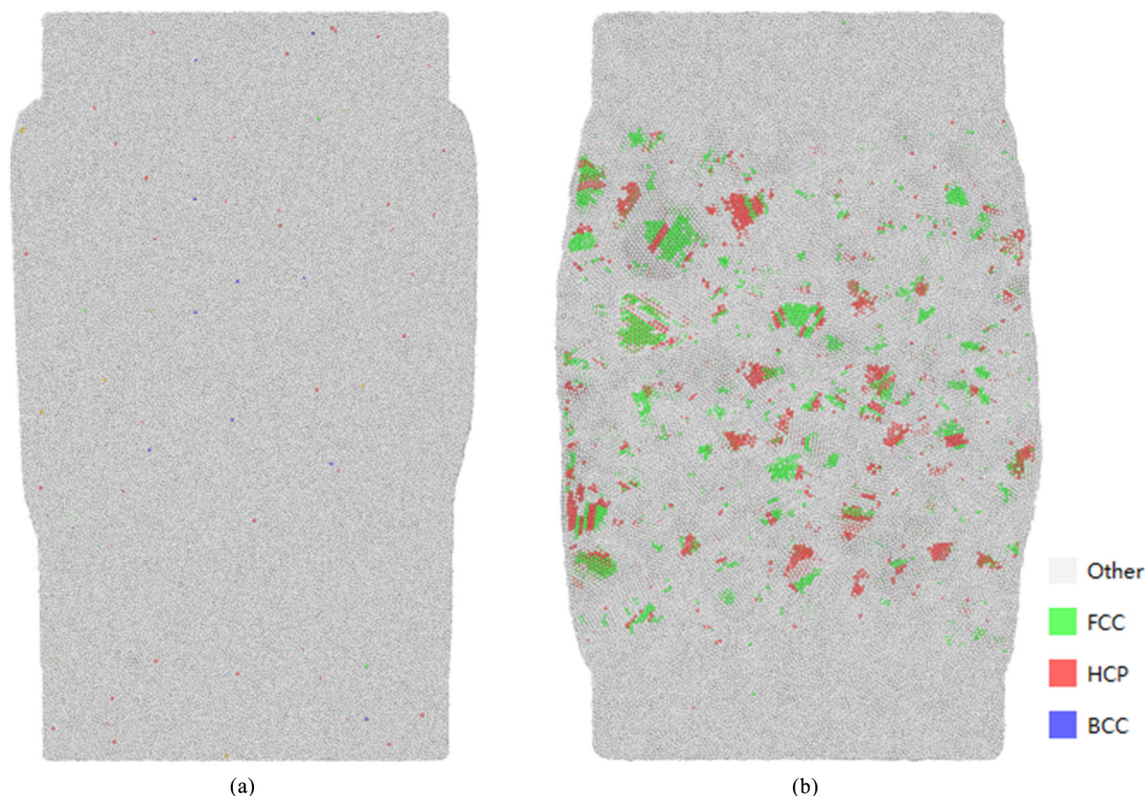


**Figure 4.** The CNA structure analysis for (a)  $Zr_{70}Cu_{30}$  and (b)  $Zr_{70}$  MGs when strain is 7%.

#### 4. Conclusions

The effect of forming pores on the plasticity of  $Zr_{70}Cu_{30}$  metallic glasses was studied. Simulation reproduces the images of the evolution of pores in the metallic glass. Our results indicate that forming porosity in  $Zr_{70}Cu_{30}$  metallic glasses can enhance the glass plasticity significantly. The enhancement of plasticity is attributed to large amount of randomly distributed free space. And it can also promote forming crystalline

phases in amorphous matrix. The simulation results are in good agreement with experimental results.

#### Acknowledgements

We thank Shaopeng Pan from Peking University for helpful program analysis. This work was supported by the National Basic Research Program of China (2013CB733000) and the National Natural Science Foundation of China (51271161 and 51271162).

#### References

1. Wang WH. The elastic properties, elastic models and elastic perspectives of metallic glasses. *Progress in Materials Science*. 2012; 57(3):487-656. <http://dx.doi.org/10.1016/j.pmatsci.2011.07.001>.
2. Pekarskaya E, Kim CP and Johnson WL. *In situ* transmission electron microscopy studies of shear bands in a bulk metallic glass based composite. *Journal of Materials Research*. 2001; 16(9):2513-2518. <http://dx.doi.org/10.1557/JMR.2001.0344>.
3. Li G, Wang YY, Liaw PK, Li YC and Liu RP. Electronic structure inheritance and pressure-induced polyamorphism in lanthanide-based metallic glasses. *Physical Review Letters*. 2012; 109(12):125501. <http://dx.doi.org/10.1103/PhysRevLett.109.125501>. PMID:23005956.
4. Wang WH. Metallic glasses: family traits. *Nature Materials*. 2012; 11(4):275-276. <http://dx.doi.org/10.1038/nmat3277>. PMID:22437786.
5. Zeng Q, Sheng HW, Ding Y, Wang L, Yang WG, Jiang JZ, et al. Long-range topological order in metallic glass. *Science*. 2011; 332(6036):1404-1406. <http://dx.doi.org/10.1126/science.1200324>. PMID:21680837.
6. Wang ZT, Pan J, Li Y and Schuh CA. Densification and strain hardening of a metallic glass under tension at room temperature. *Physical Review Letters*. 2013; 111(13):135504. <http://dx.doi.org/10.1103/PhysRevLett.111.135504>. PMID:24116793.
7. Chen MW. Mechanical behavior of metallic glasses: microscopic understanding of strength and ductility. *Annual Review of Materials Research*. 2008; 38(1):445-469. <http://dx.doi.org/10.1146/annurev.matsci.38.060407.130226>.
8. Sun BA, Pauly S, Tan J, Stoica M, Wang WH, Kühn U, et al. Serrated flow and stick-slip deformation dynamics in the presence of shear-band interactions for a Zr-based metallic glass. *Acta Materialia*. 2012; 60(6):4160-4171. <http://dx.doi.org/10.1016/j.actamat.2012.04.013>.

9. Schuh CA and Nieh TG. A nanoindentation study of serrated flow in bulk metallic glasses. *Acta Materialia*. 2003; 51(1):87-99. [http://dx.doi.org/10.1016/S1359-6454\(02\)00303-8](http://dx.doi.org/10.1016/S1359-6454(02)00303-8).
10. Feng SD, Qi L, Li G, Zhao W and Liu RP. Effects of pre-introduced shear origin zones on mechanical property of ZrCu metallic glass. *Journal of Non-Crystalline Solids*. 2013; 373-374(1):1-4. <http://dx.doi.org/10.1016/j.jnoncrysol.2013.03.041>.
11. Brothers AH and Dunand DC. Ductile bulk metallic glass foams. *Advanced Materials*. 2005; 17(4):484-486. <http://dx.doi.org/10.1002/adma.200400897>.
12. Brothers AH, Scheunemann R, DeFouw JD and Dunand DC. Processing and structure of open-celled amorphous metal foams. *Scripta Materialia*. 2005; 52(4):335-339. <http://dx.doi.org/10.1016/j.scriptamat.2004.10.002>.
13. Schroers J, Veazey C and Johnson WL. Amorphous metallic foam. *Applied Physics Letters*. 2003; 82(3):370. <http://dx.doi.org/10.1063/1.1537514>.
14. Wada T and Inoue A. Formation of porous Pd-based bulk glassy alloys by a high hydrogen pressure melting-water quenching method and their mechanical properties. *Materials Transactions*. 2004; 45(8):2761-2765. <http://dx.doi.org/10.2320/matertrans.45.2761>.
15. Wada T and Inoue A. Fabrication, thermal stability and mechanical properties of porous bulk glassy Pd-Cu-Ni-P alloys. *Materials Transactions*. 2003; 44(10):2228-2231. <http://dx.doi.org/10.2320/matertrans.44.2228>.
16. Wang D, Li Y, Sun BB, Sui ML, Lu K and Ma E. Bulk metallic glass formation in the binary Cu-Zr system. *Applied Physics Letters*. 2004; 84(20):4029-4031. <http://dx.doi.org/10.1063/1.1751219>.
17. Cheng YQ, Sheng HW and Ma E. Atomic level structure in multicomponent bulk metallic glass. *Physical Review Letters*. 2009; 102(24):245501. <http://dx.doi.org/10.1103/PhysRevLett.102.245501>. PMID:19659024.
18. Cheng YQ, Cao AJ, Sheng HW and Ma E. Local order influences initiation of plastic flow in metallic glass: effects of alloy composition and sample cooling history. *Acta Materialia*. 2008; 56(18):5263-5275. <http://dx.doi.org/10.1016/j.actamat.2008.07.011>.
19. Shimizu F, Ogata S and Li J. Theory of shear banding in metallic glasses and molecular dynamics calculations. *Materials Transactions*. 2007; 48(11):2923-2927. <http://dx.doi.org/10.2320/matertrans.MJ200769>.
20. Antoniou A, Bastawros AF, Lo CCH and Biner SB. Deformation behavior of a zirconium based metallic glass during cylindrical indentation: in situ observations. *Materials Science and Engineering A*. 2005; 394(1-2):96-102. <http://dx.doi.org/10.1016/j.msea.2004.11.031>.
21. Wang H, Li R, Wu Y, Chu XM, Liu XJ, Nieh TG, et al. Plasticity improvement in a bulk metallic glass composed of an open-cell Cu foam as the skeleton. *Composites Science and Technology*. 2013; 75:49-54. <http://dx.doi.org/10.1016/j.compscitech.2012.11.017>.
22. Yang D-H, Shang-Run Y, Hui W, Ai-Bin M, Jing-Hua J, Jian-Qing C, et al. Compressive properties of cellular Mg foams fabricated by melt-foaming method. *Materials Science and Engineering A*. 2010; 527(21-22):5405-5409. <http://dx.doi.org/10.1016/j.msea.2010.05.017>.
23. Hays CC, Kim CP and Johnson WL. Microstructure controlled shear band pattern formation and enhanced plasticity of bulk metallic glasses containing *in situ* formed ductile phase dendrite dispersions. *Physical Review Letters*. 2000; 84(13):2901-2904. <http://dx.doi.org/10.1103/PhysRevLett.84.2901>. PMID:11018971.
24. Fan C, Ott RT and Hufnagel TC. Metallic glass matrix composite with precipitated ductile reinforcement. *Applied Physics Letters*. 2002; 81(6):1020. <http://dx.doi.org/10.1063/1.1498864>.
25. Hofmann DC, Suh JY, Wiest A, Duan G, Lind ML, Demetriou MD, et al. Designing metallic glass matrix composites with high toughness and tensile ductility. *Nature*. 2008; 451(7182):1085-1089. <http://dx.doi.org/10.1038/nature06598>. PMID:18305540.